concentration of 0.17 mg/mL (day -14). At days 0, 14, and 28, synovitis was reactivated by intravenous injection of 500 μL of PGPS via the tail vein. Animals were euthanized after 6 weeks. For the ACLT model, OA was induced unilaterally through anterior cruciate ligament transection and partial medial meniscectomy in the left knee of six rats and euthanized after 16 weeks. After euthanasia, knee joints were fixed in 4% formaldehyde solution, decalcified in 0.5 M ethylenediaminetetraacetic acid, embedded in paraffin, and cut into 5-μm thick coronal knee joint sections. Sections were stained with Safranin-O/fast green to determine cartilage damage using the Mankin score. H&E staining was used to evaluate synovitis using the Krenn score. OSM expression was assessed by immunohistochemistry. For quantification purposes, the stained joint sections were ranked from 0 to 3 (0 = no staining; 3 = maximum staining) based on the OSM staining intensity in the articular cartilage, periosteum, menisci, femorotibial synovium, and collateral ligaments. Scoring was done two independent observers blinded for treatment, and scores were averaged.

Results: In the PGPS model, extracellular OSM staining was observed in articular cartilage, meniscus, periosteum, and synovium (Figure 1). Additionally, intracellular staining was observed in articular chondrocytes and meniscal fibrochondrocytes. In the ACLT model, extracellular OSM staining was found in the periosteum and synovium, but not in cartilage or meniscus (Figure 1). Similarly to the PGPS model, intracellular staining was found in articular cartilage and meniscal cells. While the overall OSM score was significantly higher in PGPS-treated knees than in control knees ($p < 0.01$; Figure 2A), no differences were seen between OA or control knees in the ACLT model ($p = 0.873$). In both models, induction of OA led to increased synovitis according to the Krenn score (Figure 2B), however cartilage damage was only observed in ACLT joints ($p < 0.05$) (Figure 2C). Furthermore, the total OSM score strongly correlated with synovitis in the PGPS model ($\rho = 0.848$, $p = 0.001$, Figure 2D), but not in the ACLT model ($\rho = 0.272$, $p = 0.387$). No correlation was found between OSM expression and cartilage damage in either model (Figure 5E). Finally, osteophyte volume correlated moderately with the total OSM expression in the PGPS knees ($\rho = 0.623$, $p = 0.034$), but not in the ACLT knees ($\rho = 0.238$, $p = 0.472$) (Figure 5F).

Conclusions: We have for the first time mapped the presence of OSM in various joint tissues in two models of arthritis. OSM expression was correlated with synovial inflammation and osteophyte formation but not with cartilage damage in the PGPS model. On the other hand, although the ACLT model resulted in cartilage damage, synovial inflammation, and osteophyte formation, these parameters did not correlate with OSM expression. This data suggests that OSM presence is associated with an inflammatory arthritis phenotype, but not with instability-induced OA. To further elucidate the role of OSM in OA, future studies should focus on in vivo inhibition of OSM upon induction of OA. This knowledge may potentiate the use of OSM as a biomarker or therapeutic target for specific OA phenotypes.

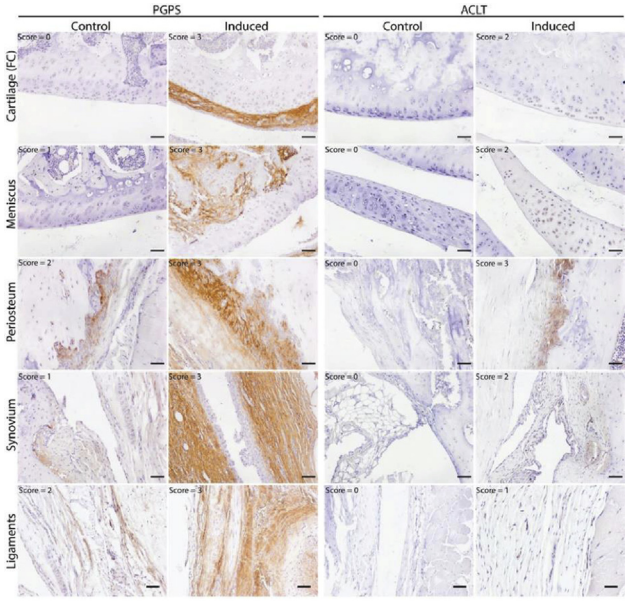

Figure 1. OSM expression pattern in acute arthritis and instability-induced OA. Representative pictures of OSM expression (brown staining) in different joint structures: Femur condyle (FC) cartilage, meniscus, periosteum and synovium. Acute arthritis in the PGPS model was induced by intra-articular injection of PGPS in the left knee. The ACLT model was induced unilaterally (left knee) through anterior cruciate ligament transection and partial medial meniscectomy. Individual scores for each structure are displayed in the top left corner of each picture. Scale bar: 50 μm.

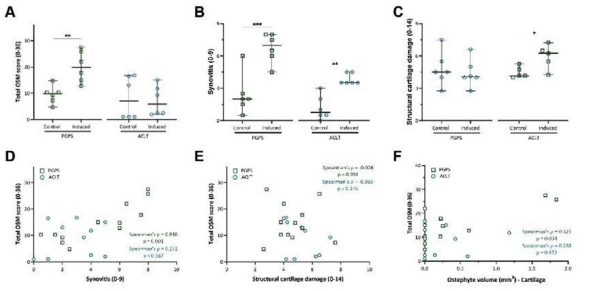

Figure 2. OSM expression and correlation with synovitis and cartilage damage. a) Total OSM score. Calculated by adding up individual scores for each compartment. b) Synovitis was scored according to the Krenn score. c) Cartilage damage was scored according to the Mankin score. Data are presented as median and 95% CI. Each individual data point represents a rat knee. (*: $p < 0.05$, **: $p < 0.01$ and ***: $p < 0.001$). c) Correlation scatterplot between total OSM staining and synovitis score in both PGPS and ACLT models. e) Correlation scatterplot between total OSM staining and articular cartilage damage in both PGPSand ACLT models. f) Correlation scatterplot between total OSM and osteophyte volume in both PGPS and ACLT models. Each individual data point represents a rat knee.

480

EVALUATION OF CD34^{+} HEMATOPOIETIC STEM CELL-ASSOCIATED EXTRACELLULAR VESICLES AS A POTENTIAL PERSONALIZED THERAPY FOR OSTEOARTHRITIS

X. Zhang [1], M.-F. Hsueh [1], V.B. Kraus [2]. [1] *Duke Molecular Physiology Inst., Dept. of Orthopaedic Surgery, Duke Univ. Sch. of Med., Duke Univ., Durham, NC, USA;* [2] *Duke Molecular Physiology Inst., Dept. of Med., Duke Univ. Sch. of Med., Duke Univ., Durham, NC, USA*

Purpose: Platelet-rich plasma (PRP) injections for knee osteoarthritis (OA) are used increasingly in attempts to improve knee functional status and symptoms. Although platelet-derived growth factors are thought to stimulate chondrocyte proliferation, leading to cartilage repair, the mechanisms of action and main effectors of PRP are not fully understood. Plasma contains a high amount of circulating extracellular vesicles (EVs), which are released by almost all mammalian cells, including platelets and stem cells, and that carry surface markers and effectors (e.g. cytoplasmic proteins, DNA, mRNA, miRNA, small non-coding RNAs, mitochondria, and cytokines) from their parent cells. EVs have been posited to be mediators of cell-to-cell communication and paracrine effects through transfer of their cargo to recipient cells. Therefore, EVs have the potential to be therapeutic components of PRP in OA. We hypothesized that characterizing EVs in plasma and synovial fluid (SF) from OA patients and comparison to non-OA controls would aid an understanding of EV subsets that could be developed as a potential personalized therapy for OA.

Methods: Plasma samples of 16 healthy controls (HCs, mean age 68 ± 8 years, 8 male and 8 female) and 48 knee OA patients (mean age 69 ± 9 years, 24 male and 24 female) and SF samples from 48 knee OA patients (mean age 67 ± 12 years, 25 male and 23 female) were acquired under donor consent and IRB approval of Duke University. Blood and SF samples were centrifuged to remove debris, cells and platelets, and plasma and cell-free SF were stored at -80^{o}C until analysis. SF was incubated briefly with hyaluronidase to specifically cleave hyaluronic acid. EVs in plasma and SF were separated by ExoQuick and re-suspended in double filtered PBS for immunostaining with fluorescence-conjugated antibodies against human CD81, CD9, CD29, CD63, CD8, CD4, CD68, CD14, CD56, CD15, CD19, CD235a, CD41a, CD34, CD31, HLA-ABC, HLA-G and HLA-DRDPDQ. EVs were also fixed, permeabilized and immunostained with fluorescence-conjugated antibodies against intra-vesicular cytokines including IL-1β, IL-10, IFN-γ, TNF-α, IL-6, and IL-17A. The percentages of the EVs expressing each tested molecule were determined using a high-resolution multicolor BD LSR Fortessa X-20 Flow Cytometer. All statistical comparisons were planned in advance of data collection. GraphPad Prism 8.0 software was used for statistical analysis. MitoTracker™ Deep Red FM and PKH67 labeled EVs were incubated for 3 days with primary human OA chondrocyte tissue explants or synoviocytes and uptake monitored by fluorescent microscopy.

Results: We observed five discrete subsets of EVs in plasma and SF varying in diameter from extra-large (ExLEV, 1000 - 6000 nm); large

(LEV, 800 - 1000 nm); medium (MEV, 100 - 800 nm); small (SEV, 20 - 100 nm); and extra-small (ExSEV, < 20 nm). The percentage of $CD34^+$ (hematopoietic stem cell)-associated EVs in healthy control and OA plasma was high (mean range 7-14% for healthy control vs 5-13% for OA depending on EV diameter); they carried respiring mitochondria and did not decline with age. Compared with the HLA-DRDPDQ$^+$ EVs, the $CD34^+$ plasma EVs from OA patients carried lower levels of the pathogenic cytokines, TNF-alpha and IFN-γ. In addition, $CD34^+$ plasma EVs rarely co-expressed HLA-DRDPDQ. The percentages of $CD34^+$ EVs in OA SF (mean range 3-9%) were lower than OA plasma. Upon 3-day culture, fluorescent EVs were taken up ubiquitously by synoviocytes but only penetrated into chondrocytes located on the surface of cartilage explants.

Conclusions: Further research is needed to understand the biological effects of plasma $CD34^+$ EVs and the feasibility of utilizing an EV-based approach as a therapeutic strategy in OA. The plasma appears to be a good source of these EVs that might be used to boost the low SF levels. Their paucity of immunogenic surface markers may suggest low immunogenicity compared with cells or other EV types.

Acknowledgments: The authors wish to acknowledge funding support from National Institute on Aging grant 1R56AG060895-01.

Figure 1. Graphs showing representative staining of co-expression of CD34 and HLA-DRDPDQ in gated individual EV subsets from one plasma and one SF.

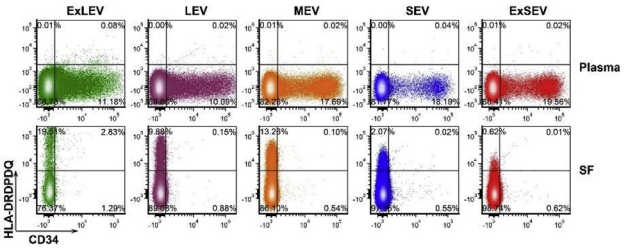

481
TRANSFORMING GROWTH FACTOR BETA VARIATION WITH PHYSICAL ACTIVITY IN KNEE OSTEOARTHRITIS

L.C. Alexander, Jr., A.J. Han, J.L. Huebner, V.B. Kraus. *Duke Univ., Durham, NC, USA*

Purpose: Transforming growth factor beta (TGF-β) is a multifunctional cytokine with three different mammalian isoforms. All three isoforms of TGF-β are secreted as inactive latent complexes. Bound to latency-associated peptide, TGF-β is unable to bind to membrane receptors. Therefore, even though TGF-β is constitutively expressed throughout the body, only the free ligand is biologically active and able to modulate the metabolic activity of cartilage. An existing theory likens the latent TGF-β complex to a molecular sensor that monitors the extracellular matrix and responds to perturbations by releasing free TGF-β. In the cartilage, TGF-β1 plays an essential role in regulating cartilage matrix metabolism. The goal of this study was to assess the effects of physical activity on free and total TGF-β isoforms in plasma from individuals with knee osteoarthritis (OA).

Methods: To assess the impact of physical activity on biomarker variation, participants (n=20; 65% female; 80% white; mean age 70 years; mean BMI 31.72 kg/m2) were recruited on the basis of symptomatic OA in at least one knee. Knee OA severity was assessed from a postero-anterior semi-flexed radiograph with a SynaFlexer positioning device and quantified by Kellgren Lawrence (K-L) score for each knee. Blood was obtained at 4 different time points (Figure 1). The interval from T0 to T1A was devoted to physical activity including activities of daily living and non-brisk walking for 1 hour, with no more than 10 minutes rest at any one time. All procedures were approved by the Institutional Review Board. Using commercially available ELISA assays, we quantified free and total TGF-β1 (BioLegend) in plasma samples (n=80) and available matched serum (n=79) samples. Total TGF-β2 and TGF-β3 (MSD U-PLEX ELISA) were also quantified in plasma (n=80). The data for TGF-β3 should be interpreted with caution, as 47.5% of samples had concentrations below the LLOD so were imputed as 1/2 LLOD for analyses. To assess variations in TGF-β over this time period, biomarker concentrations for the four time points were normalized to the mean across all four time points for each individual. Significance was assessed by non-parametric Friedman test and Dunn's post-hoc test. Spearman correlation was used to evaluate associations between non-normalized: free and total plasma TGF-β1; serum and plasma free and total TGF-β1; all total TGF-β isoforms; and free and total TGF-β1 (T1A and change from T0 to T1A) with sum K-L grade.

Results: Median plasma concentrations (range pg/ml) were as follows: free TGF-β1: 8.53 (0-40.71); total TGF-β1: 27343.00 (6760.00-81815.00); total TGF-β2: 24.99 (0-170.30); and total TGF-β3: 1.03 (0-3.10). Free plasma TGF-β1 represented 0.032% of total plasma TGF-β1. Free and total TGF-β1, and total TGF-β2, increased significantly after one hour of activity (Figure 2; time point T0 to T1A). The mean fold-change increase with activity was 1.7 for free TGF-β1, 1.4 for total TGF-β1, and 1.5 for total TGF-β2. After food consumption (T1B), TGF-β3 concentrations decreased an average of 62% from T1A, but no significant changes occurred in the other TGF-β isoforms at this time point. In plasma, total TGF-β1 strongly correlated with free TGF-β1 (rs=0.36, p=0.008), total TGF-β2 (rs=0.69, p<0.0001), and total TGF-β3 (rs=0.36, p=0.001). Total TGF-β2 also correlated with Total TGF-β3 (rs=0.29, p=0.01). Serum TGF-β1 concentrations were consistently higher than plasma concentrations (a mean 17.5-fold for free TGF-β1 and a mean 1.6-fold for total TGF-β1). Plasma and matched sera did not correlate for free TGF-β1 (rs=0.09, p=0.43) or total TGF-β1 (rs=0.19, p=0.09). Neither free nor total TGF-β1 were associated with sum K-L grade.

Conclusions: This study demonstrates that plasma concentrations of both free and total TGF-β1, and total TGF-β2, all significantly increased with physical activity, suggesting release from a mechanically sensitive reservoir. These results are consistent with known release of TGF-β1 from extracellular matrix of myofibroblasts upon mechanical contraction in vitro. We observed an effective 1.7-fold increase of circulating free (active) TGF-β1 during an hour of activity (from a mean 8.45 to a mean 13.08 pg/ml). Based upon previous published studies, these concentrations may represent a physiologically relevant modulation. These results suggest the need for standardization of activity prior to biofluid sampling intended for TGF-β analyses to assess its impact on musculoskeletal health and disease.

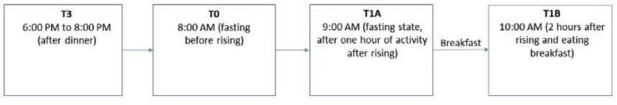

Fig. 1: Flow chart of time points for participants. Blood samples were taken at each listed time and processed.

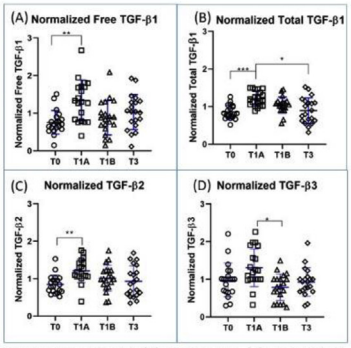

Fig. 2: Normalized data of time-points for (A) Free TGF-β1, (B) Total TGF-β1, (C) TGF-β2, (D) TGF-β3. All graphs had significant Friedman tests, and significant Dunn's post-hoc tests are indicated by brackets corresponding to the following p-values: (A) **p=0.006; (B) ***p=0.0003, *p=0.029; (C) **p=0.011; (D) *p=0.042

482
HALLMARKS OF CELLULAR SENESCENCE MORE ABUNDANT IN DAMAGED COMPARED TO INTACT CARTILAGE IN OSTEOARTHRITIS

Y.-H. Chen, C.-H. Chou, D. Attarian, V. Kraus. *Duke Univ., Durham, NC, USA*

Purpose: Cellular senescence is a consequence of aging, which is associated with cell cycle arrest and has recently been identified as a major factor in the pathogenesis of osteoarthritis. Senescence could